

Research Paper

Carcinogenic Role and Clinical Significance of Histone H3-H4 Chaperone Anti-silencing Function 1 B (ASF1B) in Lung Adenocarcinoma

Congkuan Song^{1#}, Yaolin Song^{2#}, Xiaoxia Wan^{2#}, Zhihong Zhao², Qing Geng^{1✉}

1. Department of Thoracic Surgery, Renmin Hospital of Wuhan University, Wuhan, China.
2. Department of Thoracic Surgery, Ezhou Central Hospital, Ezhou, China.

#These authors contributed equally to this work.

✉ Corresponding authors: **Qing Geng**, MD, Department of Thoracic Surgery, Renmin Hospital of Wuhan University, No.238 Jiefang Road, Wuchang District, Wuhan 430060, China; Telephone number: +86-27-8804-1919; Fax number: +86-27-8807-2292; E-mail address: gengqingwhu@whu.edu.cn. **Zhihong Zhao**, Department of Thoracic Surgery, Ezhou Central Hospital, No.9 Wenxing Road, Echeng District, Ezhou 436000, China; Telephone number: +86-27-60660425; E-mail address: 546295164@qq.com.

© The author(s). This is an open access article distributed under the terms of the Creative Commons Attribution License (<https://creativecommons.org/licenses/by/4.0/>). See <http://ivyspring.com/terms> for full terms and conditions.

Received: 2023.08.02; Accepted: 2023.09.25; Published: 2024.01.01

Abstract

Histone H3-H4 chaperone anti-silencing function 1 (ASF1) plays an important role in the polymerization, transport, and modification of histones. However, the significance of ASF1B in lung adenocarcinoma (LUAD) is largely overlooked. We investigated the aberrant expression of ASF1B in LUAD and its potential link to patient survival using multiple databases. ASF1B-overexpressing and knockdown cell lines were constructed to explore its effects on the biological behavior of lung cancer cells. ssGSEA, TMB, TIDE and IMvigor210 cohort were used to explore and validate the association of ASF1B to tumor immunity. Our data suggested that ASF1B was overexpressed in LUAD, and was associated with poor prognosis. ASF1B promoted the proliferation, migration, and invasion of lung cancer cells by regulating the phosphorylation of AKT *in vitro*. ASF1B was associated with tumor immunity. In summary, ASF1B may promote malignant behavior of LUAD cells, and its overexpression correlates with worse prognosis and better immunotherapy effect.

Keywords: Anti-silencing function 1B (ASF1B), lung adenocarcinoma (LUAD), prognosis, immunotherapy, biomarker.

Introduction

Lung cancer is one of the malignant tumors with high morbidity and mortality, with complex and diverse etiology [1]. Lung adenocarcinoma (LUAD) is the most common form of non-small cell lung cancer (NSCLC), accounting for approximately 40% of lung cancer cases [2]. Clinically, patients with LUAD often lack typical clinical symptoms or even have no symptoms in the early stage, and LUAD are prone to distant metastasis and high drug resistance. These characteristics also make the clinical treatment of LUAD extremely challenging. The treatment of lung cancer is mainly surgery, radiotherapy and chemotherapy. In recent years, with the rapid development of medicine, the treatment methods of lung cancer are gradually enriched, and gene targeted therapy and

immunotherapy are also gradually emerging. Despite the importance of these new therapies for improving patient outcomes, some patients with LUAD still lack responses to these or inevitably develop drug resistance with poor prognosis. Therefore, further studies are still necessary to better understand the mechanisms underlying the development of LUAD in order to explore more alternative treatment strategies.

The anti-silencing function 1 (ASF1), as the histone H3-H4 chaperone, was initially identified in yeast [3]. It plays an important role in histone polymerization, transport, modification and other processes, as well as in DNA replication, DNA damage repair and transcriptional regulation [4-7]. Previous studies [8, 9] have shown that ASF1B is

dysregulated in multiple malignancies and can regulate cell proliferation, apoptosis and cell cycle. However, its expression pattern, molecular mechanisms and clinical significance in LUAD are not fully understood. Here, we performed a systematic analysis of ASF1B using multiple databases, explored the expression of ASF1B in different cancers and its association with prognosis, and highlighted the importance of ASF1B in LUAD. Moreover, we induced the downregulation and overexpression of ASF1B in LUAD cell lines, examined its effects on the biological behavior of lung cancer cells *in vitro*, and preliminarily revealed the molecular mechanism that ASF1B can promote malignant behavior of LUAD cells by affecting the phosphorylation of AKT. Finally, we also explored the potential associations between ASF1B expression levels and tumor immune infiltration as well as the efficacy of immunotherapy. Taken all together, our data further confirm the importance of ASF1B in LUAD and provide new insights into the role of ASF1B in the prognosis and immunity in LUAD.

Materials and Methods

Data Acquisition

From the Cancer Genome Atlas (TCGA) database (<https://cancergenome.nih.gov>), we downloaded LUAD data, including the transcriptional profile data of 535 tumor tissues and 35 normal lung tissues and the corresponding clinical data. The LUAD gene expression profiles were also downloaded from the Gene Expression Omnibus (GEO) (<https://www.ncbi.nlm.nih.gov/>). ASF1B differentially expressed in lung tumor tissues versus normal tissues was examined using the follow three datasets: TCGA-LUAD, GSE10072 [10] and GSE32863 [11]. In order to determine the impact of ASF1B on LUAD prognosis, these datasets including TCGA-LUAD, GSE30219 [12], GSE31210 [13, 14], GSE42127 [15, 16], GSE68465 [17], and GSE72094 [18] were employed. We obtained tumor and adjacent tissue specimens from 12 LUAD patients admitted to the Renmin Hospital of Wuhan University in June 2023. Acquisition of these specimens was approved by the Ethical Review Board of Renmin Hospital of Wuhan University (Approval No.: WDRY2023-K112). Furthermore, protein expression difference of ASF1B between lung tumor tissues and normal tissues was validated using the Human Protein Atlas (HPA) database (<http://www.proteinatlas.org/>) and UALCAN (<http://ualcan.path.uab.edu/>). In addition, the subcellular proteome of ASF1B was also investigated in the HPA database.

Pan-cancer analysis

ASF1B expression in pan-cancers was explored in TIMER2 database (<http://timer.cistrome.org/>). The effect of ASF1B on the prognosis of pan-cancer was analyzed in GEPIA2 webserver (<http://gepia2.cancer-pku.cn/>). The correlation of ASF1B with the immune checkpoint was explored in TISIDB database (<http://cis.hku.hk/TISIDB/>).

ssGSEA analysis for immune cells and immune pathways

Single-sample gene set enrichment analysis (ssGSEA) was conducted to quantify the score of 16 immune cells and 13 immune-related pathways or functions. Wilcoxon test was conducted to compare the immune cell and immune function scores between high and low ASF1B expression groups. The relationship between ASF1B and these scores was also examined using Spearman correlation analysis by Xiantao webserver (<https://www.xiantaozi.com/>).

Cell culture

LUAD A549 cells and human normal epithelial cells of lung (Beas-2B) were obtained from ATCC. Fetal bovine serum (FBS) were purchased from Gibco, USA. And penicillin/streptomycin and RPMI 1640 medium were from Servicebio, Wuhan. A549 cells were cultured using RPMI 1640 medium containing 10% FBS, 50 mg/mL streptomycin and 50 IU/mL penicillin, and placed in an incubator conditioned at 37°C, 5% CO₂. The solution was changed every 1~2 d, and when the cell fusion reached 80%~90%, it was digested with trypsin and passaged at 1:3.

Construction of the ASF1B-overexpressing and knockdown cell lines

According to the human ASF1B gene sequence published by GenBank, we used an online software (<https://www.ncbi.nlm.nih.gov/tools/primer-blast/>) to design the corresponding primers, the target gene fragments were amplified by nested PCR, and the vector (pHAGE-3xflag) was then digested and purified. The recombinant vector was obtained by connecting the target gene fragment with the vector. They were subsequently transferred into E. coli. We screened the positive clones for expanded culture. PEI transfection reagent (sigma, # GF95977287), 0.5µg pMD2.G (addgene, plasmid #12259 pMD2.G), and 0.75µg psPAX2 (addgene, plasmid #12260 psPAX2) were thoroughly mixed, and then mixed with 1µg target gene plasmid or control vector plasmid respectively for 15 minutes, and then added to 293T cell culture medium for lentiviral packaging. The sequences of the short hairpin RNA against human ASF1B (ASF1B-sh#1, and ASF1B-sh#2) were

respectively 5'-CTGGAGTGGGAAGATCATTAT-3' and 5'-TTAGTTAGTAGGTAGACTTAG-3'. After 6 hours of packaging the virus, the liquid in the medium was changed. After 48 hours, the virus was collected and centrifuged for 3 minutes at 12000 rpm in a centrifuge, and then collected using filter membrane with a 0.45 μm pore size. The virus collected above was added to the A549 cell culture dish to infect the target cells, and 8 $\mu\text{g}/\text{mL}$ polybrene (Sigma, H9268) was added to the two cell culture dishes respectively. After the cells were passaged, 4 $\mu\text{g}/\text{mL}$ puromycin reagent was used for screening the stably transduced cells, and the screening time was 48h.

CCK-8 Assay

The cells were plated in 96-well plates ($5 \times 10^3/\text{well}$). We added 10 μL of CCK-8 (Servicebio, Wuhan) solution to the cell culture at each time point, and the cells were incubated for 2-4h at 37 °C and 5% CO_2 . We used a microplate reader to detect the absorbance value (OD value) in each well at 450 nm.

EdU Assay

The stable ASF1B-overexpressing or knockdown cell lines with good growth status were seeded in 48-well plates with 10000 cells per well and cultured in an incubator at 37°C and 5% CO_2 . When cells had been incubated with EdU (EdU kit were purchased from Servicebio, Wuhan) for 2 hours, the culture medium was removed, and paraformaldehyde was added to fix it at room temperature for 15 min. We washed the cells thrice with PBS. Next, we added 0.3% Triton X-100 permeable solution into each well. The cells were incubated at room temperature for 15 min and then washed with PBS for 3 times. After this, we added click reaction solution to each well. And the cells were incubated at 37°C for 30 min away from light. We subsequently aspirated the click reaction solution, and washed the cells thrice with PBS. Nuclei staining was performed using Hoechst 33342.

Transwell assay

Cell migration and invasion were measured by transwell assay. Matrigel glue, and Transwell culture plates were purchased from BD, USA. Cultured cells with good growth status were harvested and made single cell suspension after tryptic digestion. We added 100 μL of cell suspension to the transwell chamber for 14 h. Subsequently, we washed the chamber twice with calcium-free PBS. After paraformaldehyde fixation and crystal violet staining, we randomly selected five fields of view under a 100-fold or 200-fold microscope to observe the cells, and the number of migrated cells was counted. For the invasion assay, matrigel was added early in the

upper chamber of a transwell chamber and incubated in the cell incubator for about 2 h. In the upper compartments of the transwell chamber, 100 μL of cell suspension was inoculated. And the lower compartments of the transwell chamber were filled with 600 μL of RPMI 1640 medium containing 20% FBS. The cells in the upper compartment were incubated at 37 °C for 24 h, then wiped with a wet cotton swab, fixed with 4% paraformaldehyde for 10 minutes, and stained with 0.5% crystal violet for 5 minutes. In order to observe if cells entered the bottom cavity via the pore, a microscope (Olympus, Japan) was used. And these images were taken and the number of cells was counted as well.

Quantitative real-time polymerase chain reaction (qRT-PCR)

ASF1B mRNA expression in cells was measured using qRT-PCR analysis. Trizol reagents, qRT-PCR kit, and reverse transcription kit were purchased from Servicebio, Wuhan. Applying the Trizol method, the total RNA was extracted and subsequently used to synthesize cDNA and subjected to PCR reactions (all experimental procedures were performed strictly according to the instructions of the kit). β -ACTIN was used as the reference gene and relative gene expression was calculated by the $2^{-\Delta\Delta\text{CT}}$ method.

Western blot

In this experiment, we lysed cells for 30 minutes, centrifuged them, and absorbed the supernatant to extract total cellular protein. And the protein was quantitated using the BCA protein assay kit. Protein signals were detected by a BioRad ChemiDoc XRS+System. Relative protein expression levels were quantitated using β -actin as the internal reference. The relevant antibodies (ASF1B, AKT, p-AKT, β -actin) and MK2206 (#SF2712, an AKT-specific inhibitor) were purchased from Servicebio, Wuhan.

Evaluation of the immunotherapy efficacy

There is a close relationship between immunotherapy effect and immune checkpoint expression, as well as tumor mutation burden (TMB), thus we also investigated the Spearman correlation between ASF1B and some immune checkpoints in GEPIA2 webserver, and compared the differences in TMB between high and low ASF1B expression groups. TCGA somatic mutation data were also collected from the TCGA GDC (<https://portal.gdc.cancer.gov/>). Additionally, due to tumour immune dysfunction and exclusion (TIDE) integrates the characteristics of T cell dysfunction and exclusion, and simulates the tumor immune escape with different levels of tumor infiltrating cytotoxic T cells, and has very prominent advantages over other biomarkers [19], we thus

utilized the TIDE score from TIDE database (<http://tide.dfci.harvard.edu>) to predict the potential immunotherapy response. Furthermore, we obtained an immunotherapy dataset (IMvigor210) with a large sample size from a previous study [20] to further clarify the association between ASF1B expression and the immunotherapy effect.

Statistical Analysis

All statistical analyses were performed in R 3.6.2 software, Graphpad Pism9.5, IBM SPSS Statistics 23.0 and online databases. Spearman method was used for correlation analysis. The median of ASF1B expression values for all samples was used as the cut-off for grouping (high and low ASF1B expression groups). “*” or “#” in Figures represents p-value less than 0.05, “**” or “##” represents p-value less than 0.01, “***” or “###” represents p-value less than 0.001. Kaplan-Meier curves were used to assess survival outcomes, and log-rank test was performed. P-value < 0.05 was considered statistically significant.

Results

Expression and relationship with prognosis of ASF1B in human cancer

In TIMER2 analysis, we observed that ASF1B expression was dysregulated in multiple human cancers, including urinary system malignancies (bladder urothelial carcinoma (BLCA), kidney chromophobe (KICH), kidney renal clear cell

carcinoma (KIRC), and kidney renal papillary cell carcinoma (KIRP)), digestive system malignancies (cholangiocarcinoma (CHOL), liver hepatocellular carcinoma (LIHC), pancreatic adenocarcinoma (PRAD), esophageal carcinoma (ESCA), stomach adenocarcinoma (STAD), colon adenocarcinoma (COAD), and rectum adenocarcinoma (READ)), nervous system malignancies (glioblastoma multiforme (GBM), brain lower grade glioma (LGG)), respiratory system malignancies (LUAD, lung squamous cell carcinoma (LUSC)), female reproductive system malignancies (cervical squamous cell carcinoma and endocervical adenocarcinoma (CESC), uterine corpus endometrial carcinoma (UCEC)), and breast invasive carcinoma (BRCA), head and neck squamous cell carcinoma (HNSC), and thyroid carcinoma (THCA). Surprisingly, in all of these 20 human cancers, ASF1B was highly expressed (Figure 1A). Subsequently, we investigated the effect of ASF1B expression on cancer prognosis. In GEPIA2 analysis, we found that ASF1B expression could significantly affect the survival of 13 cancers. For example, ASF1B overexpression was associated with worse prognosis in some cancers, including Adrenocortical carcinoma (ACC), KIRP, KIRC, and LUAD. Instead, ASF1B overexpression was associated with better prognosis in CESC, LUSC, and STAD (Figure 1B and Figure 1S). Overall, ASF1B is upregulated in a variety of human cancers, and is closely related to their prognosis.

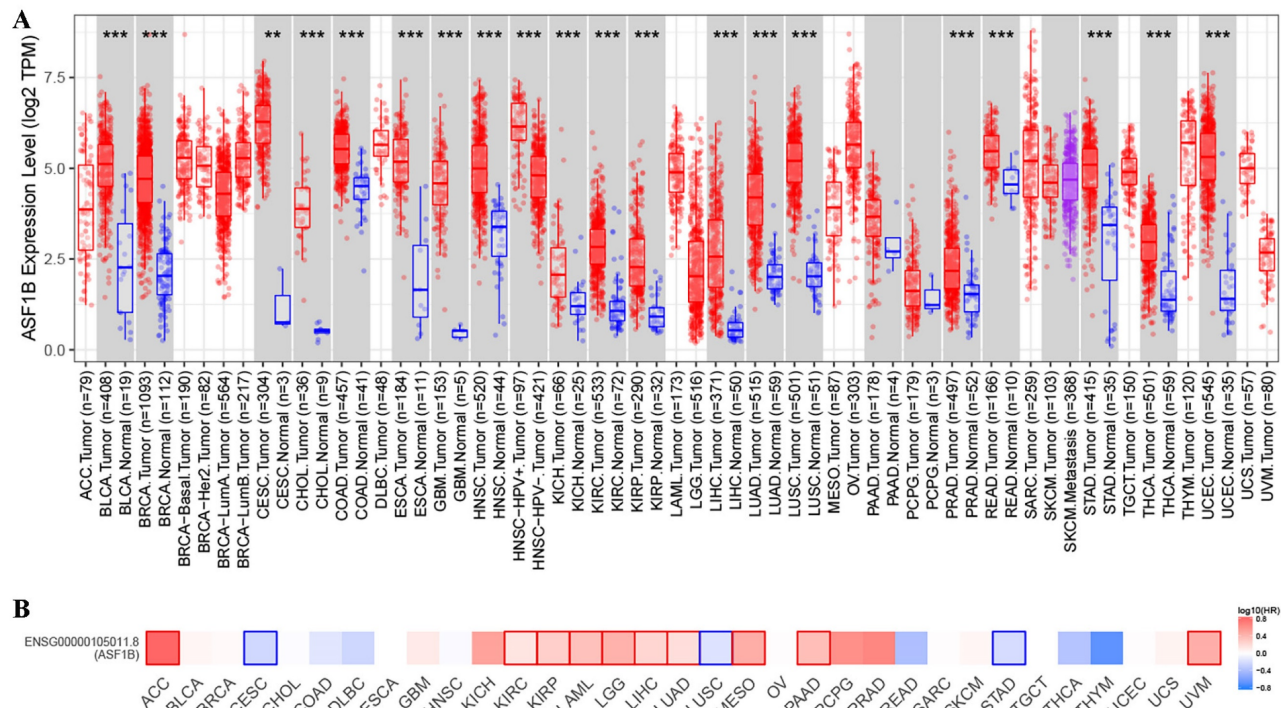


Figure 1. ASF1B expression in pan-cancer and its relationship with prognosis. (A) TIMER2 analysis revealed ASF1B expression in human pan-cancer. “***” in Figure represents p-value less than 0.05, “**” represents p-value less than 0.01, “*” represents p-value less than 0.001. **(B)** GEPIA2 analysis revealed the relationship between the expression of ASF1B and the patient outcome.

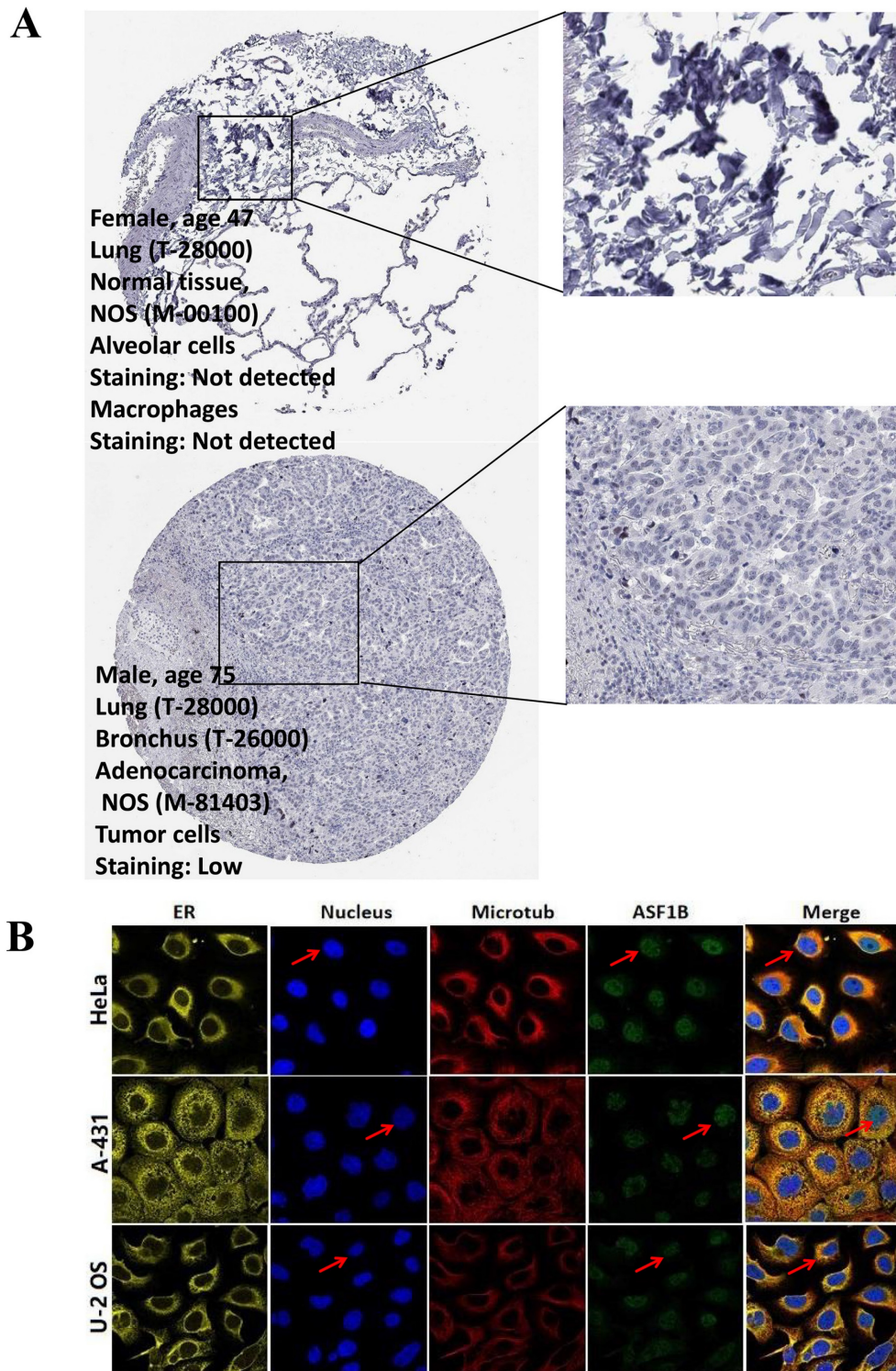


Figure 2. The immunohistochemical results and subcellular proteome of ASF1B. (A) The immunohistochemical results of ASF1B in LUAD tumor and normal tissues from HPA. **(B)** HPA database analysis revealed the subcellular proteome of ASF1B in human cancer cells (HeLa, A-431, and U-2 OS cells).

ASF1B is highly expressed in LUAD and correlates with poor prognosis

In the pan-cancer analysis described above, we initially observed the overexpressed status of ASF1B in LUAD and it was related to poor prognosis. To further clarify this relationship, we performed the

validation in multiple datasets. In the TCGA-LUAD project, we first compared ASF1B expression between the two groups in unpaired LUAD tumor (n=535) and normal tissue samples (n=59), and found that compared to normal tissues, tumor tissues expressed significantly more ASF1B. In the 57 paired LUAD tumor and normal tissue samples, as expected, ASF1B

remained highly expressed in the tumor tissue (**Figure S2A**). Similar results were seen in other data cohorts before and after the paired samples, including GSE10072 (**Figure S2B**) and GSE32863 (**Figure S2C**). At the cellular level, we also found that ASF1B expression was also significantly higher in LUAD cells compared to lung normal cells (**Figure S2D**). Similarly, ASF1B also showed significant expression differences in 12 pairs of LUAD tumors and adjacent normal tissues (**Figure S2E**). We also explored ASF1B expression at the protein level. In HPA analysis, we found that the expression level of ASF1B in tumors was higher than that in normal tissues (**Figure 2A**). From the results of immunohistochemistry, ASF1B is mainly expressed in the nucleus (**Figure 2A**). We also observed the same phenomenon (localized to the nucleoplasm) in human cancer cells (HeLa, A-431, and U-2 OS cells) in the HPA database (**Figure 2B**). Furthermore, we also observed protein expression level of ASF1B in tumors was higher than that in normal tissues (CPTAC samples) in UALCAN portal (**Figure S2F**). Similarly, we also verified the relationship between ASF1B and LUAD prognosis in multiple datasets. First, in TCGA-LUAD program, we found that the ASF1B overexpression was correlated with worse prognoses (**Figure 3A**), which was also confirmed in the subsequent TCGA subgroup analysis in multiple subsets, including age > 65y group, female group, stage T1&T2 group, stage T3&T4 group, and stage M0 group (**Figure 3B**). Similar results were seen in other LUAD cohorts, including GSE30219 (**Figure 3C**), GSE31210 (**Figure 3D**), GSE42127 (**Figure 3E**), GSE68465 (**Figure 3F**), and GSE72094 (**Figure 3G**). Moreover, to further

investigate the association between ASF1B and clinical features, we found significant correlations between ASF1B expression and patient age, T stage, N stage, and TNM stage (**Table 1**). Together, these data confirm that ASF1B is overexpressed in LUAD and correlates with poor prognosis.

Table 1. Basic information of the included patients with lung adenocarcinoma from TCGA.

Characteristics	Low expression of ASF1B	High expression of ASF1B	P value
Age, n (%)			0.035
<= 65	117 (22.5%)	140 (26.9%)	
> 65	144 (27.7%)	119 (22.9%)	
Gender, n (%)			0.179
Female	152 (28.2%)	137 (25.4%)	
Male	117 (21.7%)	133 (24.7%)	
Smoker, n (%)			0.779
No	37 (7%)	40 (7.6%)	
Yes	223 (42.5%)	225 (42.9%)	
Pathologic T stage, n (%)			0.031
T1	102 (19%)	74 (13.8%)	
T2	134 (25%)	158 (29.5%)	
T3&T4	31 (5.8%)	37 (6.9%)	
Pathologic N stage, n (%)			0.004
N0	189 (36.1%)	161 (30.8%)	
N1	39 (7.5%)	58 (11.1%)	
N2&N3	28 (5.4%)	48 (9.2%)	
Pathologic M stage, n (%)			0.079
M0	183 (46.9%)	182 (46.7%)	
M1	8 (2.1%)	17 (4.4%)	
Pathologic stage, n (%)			0.001
Stage I	169 (31.8%)	127 (23.9%)	
Stage II	53 (10%)	72 (13.6%)	
Stage III	32 (6%)	52 (9.8%)	
Stage IV	9 (1.7%)	17 (3.2%)	

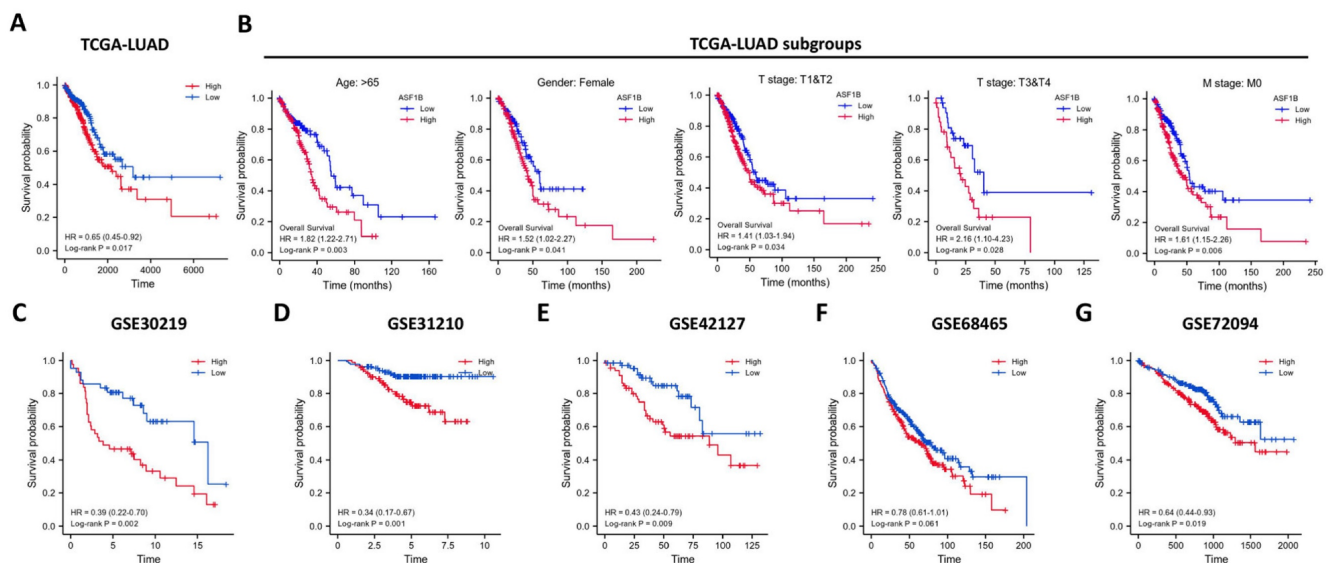


Figure 3. Effect of ASF1B expression on patient overall survival. **(A)** Kaplan-Meier curve reveals the relationship between ASF1B and the overall survival of all patients from TCGA-LUAD. **(B)** Kaplan-Meier survival curves based on TCGA-LUAD subgroups for age greater than 65 years, female patients, T1/T2, T3/T4, and stage M0. **(C-G)** Kaplan-Meier curve reveals the relationship between ASF1B and the overall survival of LUAD patients in the GEO datasets: GSE30219 **(C)**, GSE31210 **(D)**, GSE42127 **(E)**, GSE68465 **(F)** and GSE72094 **(G)**.

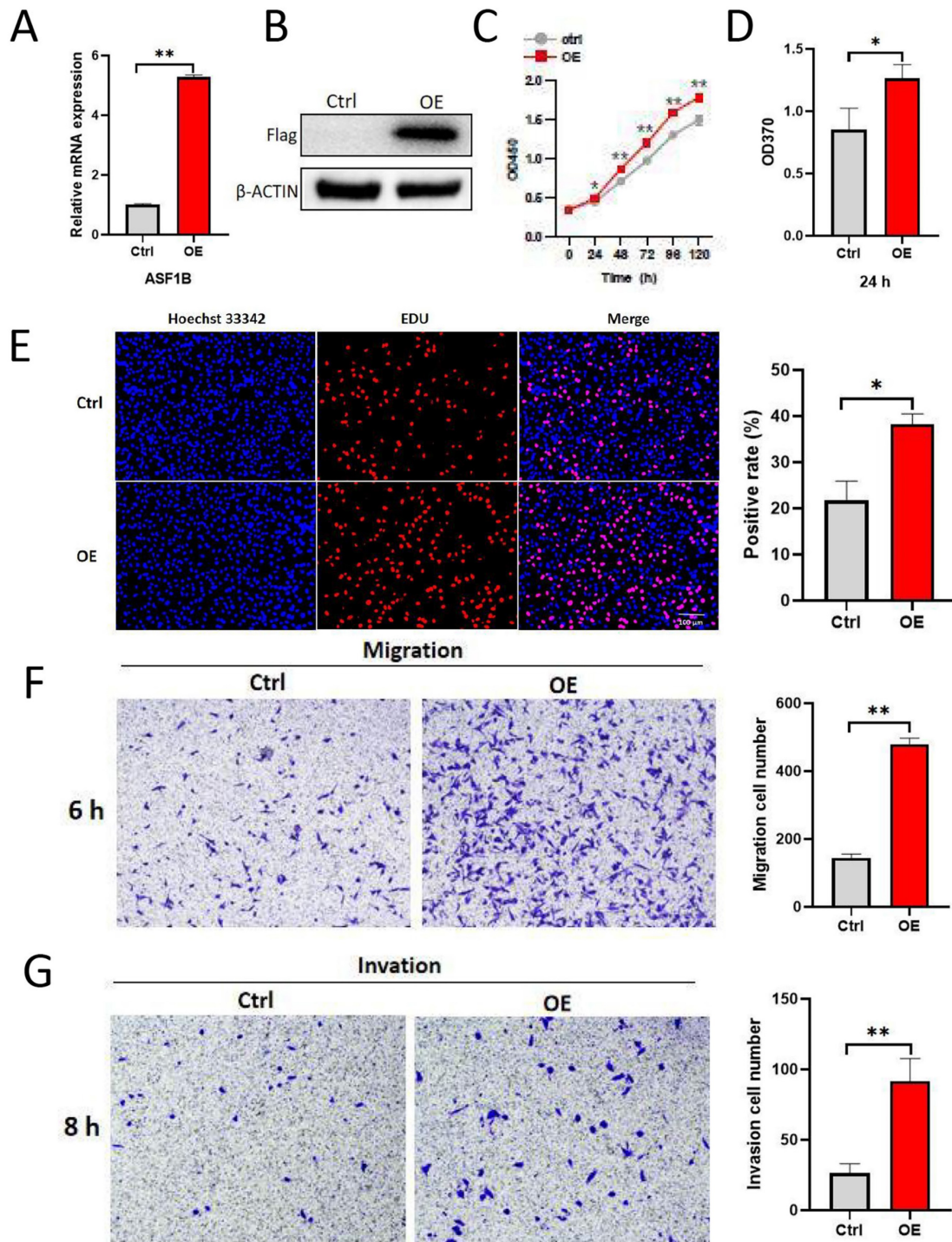


Figure 4. ASF1B overexpression promotes the proliferation, migration and invasion of lung cancer cells. (A) qRT-PCR revealed the mRNA expression levels of ASF1B in overexpressed cell lines versus control groups. (B) Western blot revealed the protein expression levels of ASF1B in overexpressed cell lines versus control groups. (C) CCK-8 assay showed the growth rate of ASF1B-overexpressing cells increased significantly with increasing time points. (D) BrdU assay revealed the OD value at 370 nm between the ASF1B overexpression and the control group cells at 24 h. (E) EdU assay revealed the cell proliferation in ASF1B overexpressed cell lines versus control groups. (F) Transwell assay revealed the migratory abilities of A549 cells. (G) Transwell assay revealed the invasive abilities of A549 cells (* $p < 0.05$, ** $p < 0.01$, *** $p < 0.001$).

ASF1B promotes the proliferation, migration, and invasion of lung cancer cells

To explore the impact of ASF1B on the biological behavior of lung cancer cells, ASF1B was overexpressed to construct stably expressed cell lines in A549. As shown in **Figure 4A-B**, ASF1B in this cell

line was significantly overexpressed at the mRNA and protein levels. The result from CCK-8 assay (**Figure 4C**) showed the growth rate of ASF1B-overexpressing cell lines increased significantly with increasing time points, and BrdU assay (**Figure 4D**) also showed that the proliferative capacity of the A549 cell lines with ASF1B

overexpression were significantly enhanced. These data suggested that ASF1B may act as an oncogene to promote lung cancer cell growth. Furthermore, to further confirm this finding, we also assessed the effect of ASF1B overexpression on lung cancer cell proliferation by EdU marker staining. As shown in **Figure 4E**, compared to the cells in the control group, ASF1B-overexpressing cells had a significantly higher positive rate for EdU staining, indicating that ASF1B overexpression can promote the proliferation of lung

cancer cells. Since lung cancer is predisposed to invasion and metastasis, we used the Transwell assay to evaluate the effect of ASF1B on the migratory and invasive ability of lung cancer cells. ASF1B overexpressing cells significantly promoted the ability of tumor cells to penetrate the transwell compartment when compared with controls (**Figure 4F**). In addition, in the invasive cell experimental model, the overexpression of ASF1B also aggravated the cell invasive ability (**Figure 4G**).

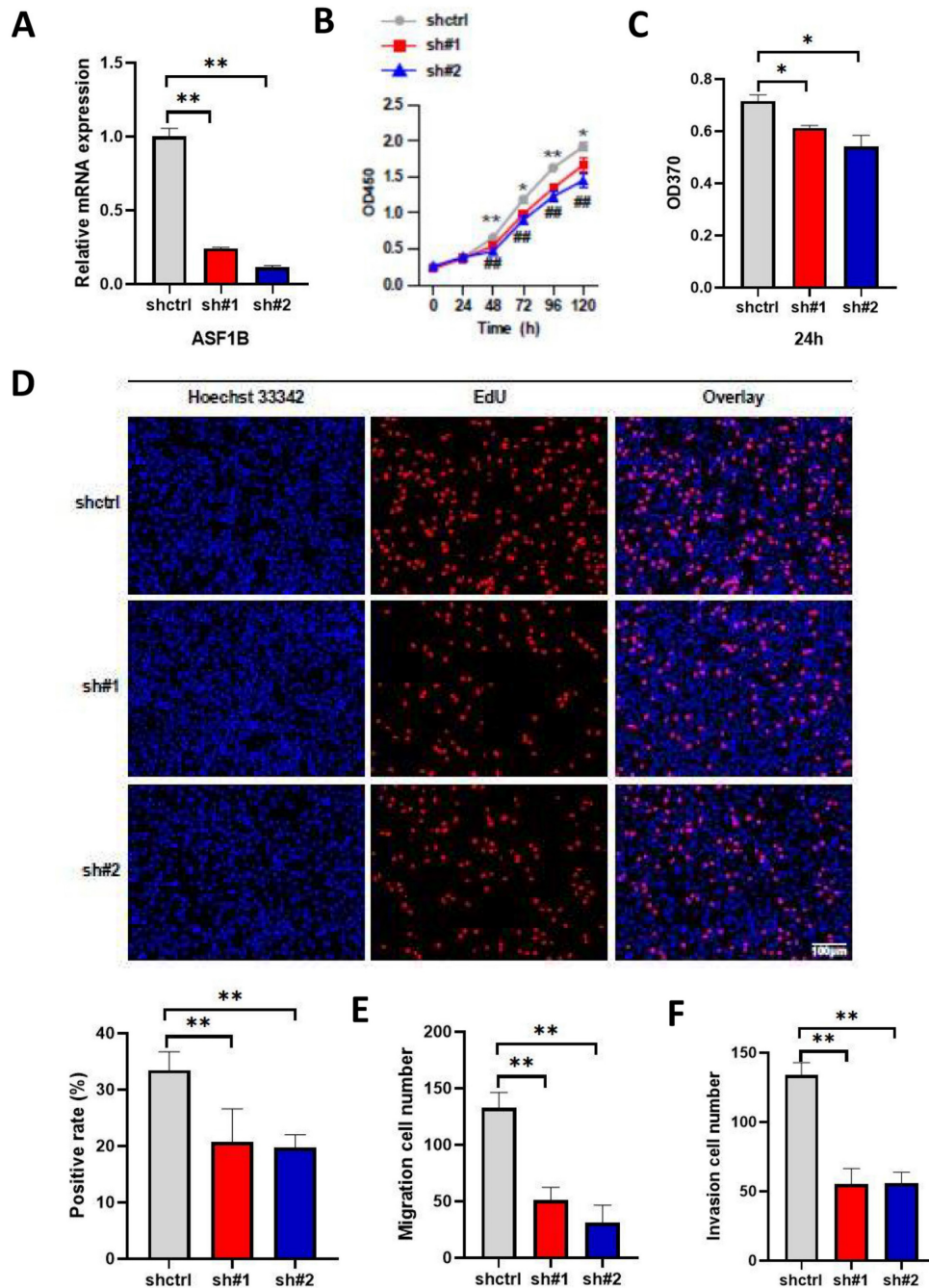


Figure 5. ASF1B knockdown inhibits the proliferation, migration, and invasion of lung cancer cells. (A) qRT-PCR revealed the mRNA expression levels of ASF1B in knockdown cell lines versus control groups. (B) CCK-8 assay showed the growth rate of ASF1B-knockdown cells decreased significantly with increasing time points (shctrl Vs. sh#1: * $p < 0.05$, ** $p < 0.01$, *** $p < 0.001$; shctrl Vs. sh#2: # $p < 0.05$, ## $p < 0.01$, ### $p < 0.001$). (C) BrdU assay revealed the OD value at 370 nm between the ASF1B knockdown and the control group cells at 24 h. (D) EdU assay revealed the cell proliferation in ASF1B-knockdown cell lines versus control groups. (E) Transwell assay revealed the migratory abilities of A549 cells. (F) Transwell assay revealed the invasive abilities of A549 cells (* $p < 0.05$, ** $p < 0.01$, *** $p < 0.001$).

The above results suggested the effect of ASF1B overexpression on the proliferation, migration, and invasion ability of lung cancer cells. To further emphasize the impact of ASF1B on the biological behavior of lung cancer cells, we constructed ASF1B-knockdown cell lines by shRNA-mediated gene silencing in A549 cell lines. This result revealed that the ASF1B expression levels were significantly decreased in the ASF1B knockdown cell lines as compared to the ASF1B non-knockdown cell lines (**Figure 5A**), suggesting the transfection was successful. The CCK-8 assay (**Figure 5B**) and BrdU assay (**Figure 5C**) showed a significant decrease in cell growth rate and proliferation capacity in the ASF1B-sh#1 and ASF1B-sh#2 cell lines. EdU marker staining (**Figure 5D**) indicated that ASF1B deletion significantly decreased the proliferation of A549 cells. These results indicated that loss of ASF1B significantly inhibited the proliferative capacity of lung cancer cells. Meanwhile, the Transwell assay was also performed to explore the effect of ASF1B deletion on cell migration and invasion. We observed a significant decrease in the number of cells that migrated in the ASF1B knockdown group (ASF1B-sh#1 and ASF1B-sh#2) (**Figure 5E-F and Figure S3**).

Overall, the above data revealed that ASF1B had

a major part to play in tumor cell proliferation, migration, and invasion. And targeting ASF1B may be a new and promising treatment strategy for LUAD.

ASF1B promotes malignant behavior of LUAD cells by regulating the phosphorylation of AKT

The PI3K/AKT pathway plays a key role in carcinogenesis, promoting cell survival and growth [21], and AKT is as the core to the PI3K/AKT pathway. To investigate whether the impact of ASF1B on the biological behavior of A549 cells was associated with AKT, we performed the following analysis. We examined the protein expression levels of AKT and phosphorylation-modified AKT (p-AKT) in lung cancer cells by Western blot. We observed that the overexpression of ASF1B significantly increased the phosphorylation level of AKT (**Figure 6A**), while the knockdown of ASF1B observably inhibited the AKT phosphorylation (**Figure 6B**). More importantly, MK2206 (an AKT-specific inhibitor), significantly inhibited the effects of ASF1B-overexpressing cell lines on tumor cell proliferation (**Figure 6C**) and migration (**Figure 6D**) *in vitro*, suggesting that AKT played a pivotal role in biological function of ASF1B in promoting lung cancer progression, and ASF1B promoted malignant behavior of LUAD cells by regulating the phosphorylation of AKT.

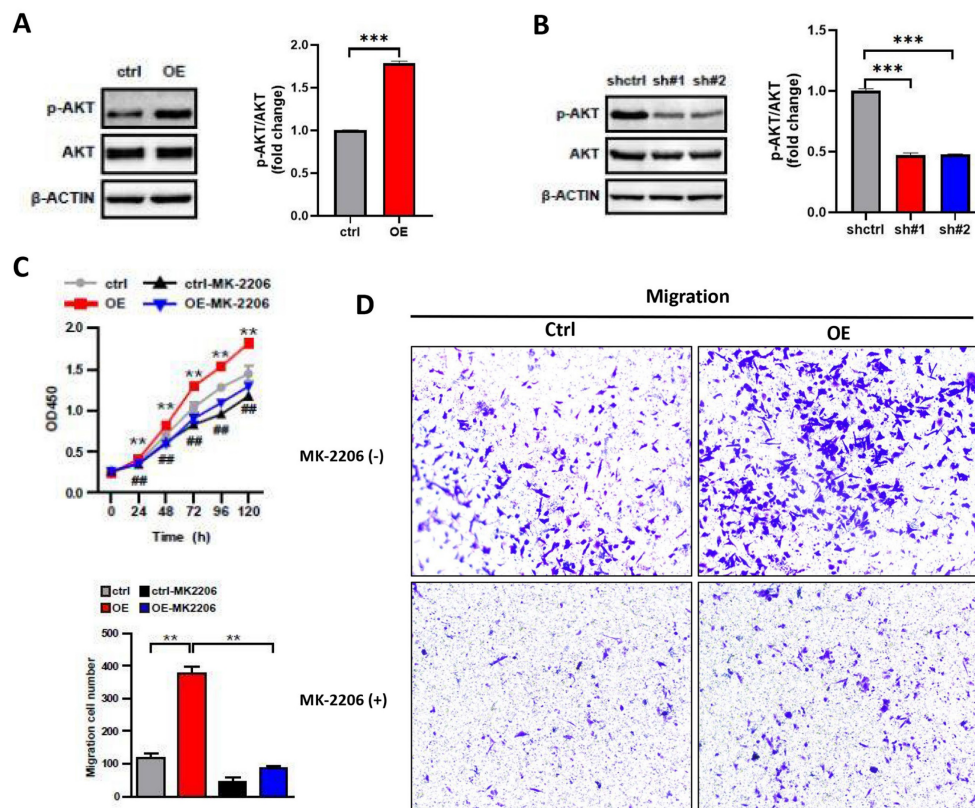


Figure 6. ASF1B promotes malignant behavior of LUAD cells by regulating the phosphorylation of AKT. (A) Western blot revealed the protein expression levels of AKT, p-AKT, β -actin in ASF1B overexpressed cell lines versus control groups. (B) Western blot revealed the protein expression levels of AKT, p-AKT, β -actin in ASF1B-knockdown cell lines versus control groups. (C) Cell activity of A549 cells in each group detected by CCK-8 (ctrl Vs. OE: * $p < 0.05$, ** $p < 0.01$, *** $p < 0.001$; ctrl Vs. Ctrl-MK-2206: # $p < 0.05$, ## $p < 0.01$, ### $p < 0.001$). (D) Migratory abilities of A549 cells in each group detected by Transwell (* $p < 0.05$, ** $p < 0.01$, *** $p < 0.001$).

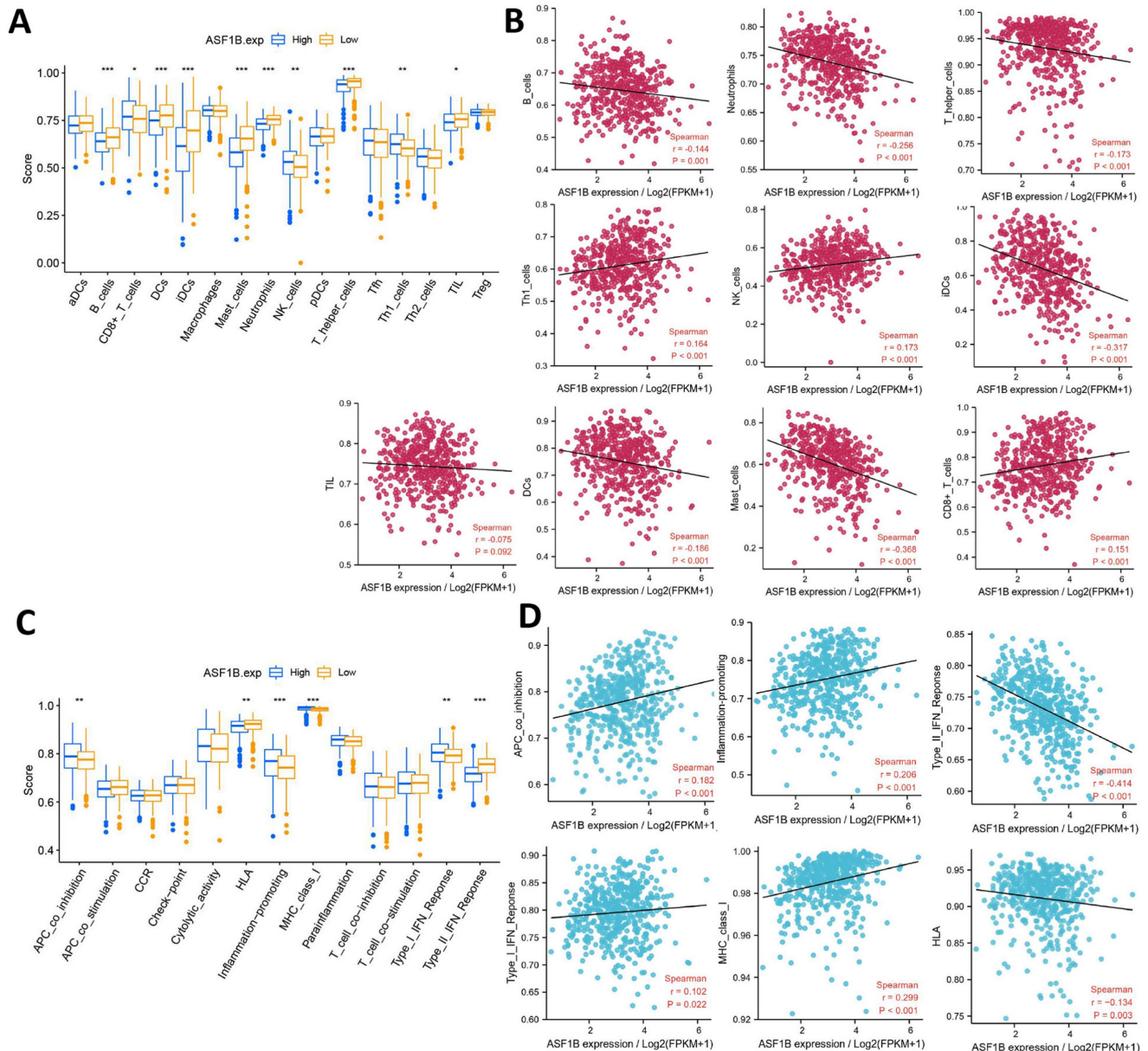


Figure 7. Correlation of ASF1B expression with immune characteristics. (A) Comparison of the abundance of immune cell infiltration between high and low ASF1B expression groups. **(B)** The relationship between ASF1B and immune cells examined by Spearman correlation analysis. **(C)** Comparison of the activity of immune-related pathways or functions between high and low ASF1B expression groups. **(D)** Spearman correlation between ASF1B expression and the activity of immune-related pathways or functions (* $p < 0.05$, ** $p < 0.01$, *** $p < 0.001$).

Correlation of ASF1B expression with immune characteristics

The relationship between ASF1B and cancer immunity is largely unknown. We thus investigated the immune characteristics of different expression groups of ASF1B using ssGSEA. Among the 16 immune cells, seven had higher infiltration abundance in the low ASF1B group, including B cells, DCs, iDCs, Mast cells, Neutrophils, TIL, T helper cells. While CD8⁺ T cells, NK cells, and Th1 cells had higher levels of infiltration in the high ASF1B group (Figure 7A). The association of these immune-infiltrating cells was also further confirmed by Spearman correlation

analysis with ASF1B (Figure 7B). In addition, among the 13 immune-related pathways, four had lower activity in the low ASF1B group, including MHC class I, APC co-inhibition, Type I IFN Response, Inflammation promoting. While HLA, Type II IFN Response displayed higher activity in the low ASF1B group (Figure 7C). Similar results were also seen in the correlation analysis of ASF1B with the activity of these immune pathways (Figure 7D).

ASF1B overexpression may indicate a better immunotherapy effect in LUAD patients

Given the above potential association of ASF1B with immunity, we were interested in further

Discussion

In the current study, we found that ASF1B expression was dysregulated (high expression state) in various human tumors. This finding was in line with previous research [22, 23]. Surprisingly, the high expression state did not correspond to their poor prognosis. For example, in CESC, LUSC, as well as STAD, ASF1B was markedly overexpressed in cancer tissues, while this overexpressed state predicted better overall survival. Existing studies have given no definite explanation, and whether this is related to the different roles of ASF1B in different cancer contexts and different stages of cancer development needs to be further studied. The study of Liu et al [24] showed that ASF1B silencing inhibited the growth of cervical cancer cells *in vivo* and *in vitro*, induced cell cycle arrest and promoted apoptosis, while ASF1B overexpression promoted the proliferation of cancer cells. This confirmed that ASF1B plays a role as an oncogene in cervical cancer cells. Similar to the study, we also found that ASF1B functions as an oncogene in LUAD. We observed high expression state of ASF1B in LUAD tumor tissues in multiple datasets (TCGA, GSE10072 and GSE32863), and this high expression state had a negative impact on patient outcome (TCGA, GSE30219, GSE31210, GSE42127, GSE68465 and GSE72094). Additionally, we found that ASF1B silencing inhibited the proliferation, migration and invasion of LUAD cells *in vitro*. On the contrary, the overexpression of ASF1B showed the opposite biological behavior in A549 cells. We speculate that this promoting effect may be related to AKT phosphorylation. AKT, a serine/threonine protein kinase, is an important downstream effector of PI3K signaling, and elevated expression of activated AKT (p-AKT) has been confirmed to be present in many human cancers, such as breast cancer [25], esophageal cancer [26], pancreatic cancer [27], lung cancer [28], etc. AKT as the core to the PI3K/AKT signaling pathway, can phosphorylate some key premalignant factors to promote cell viability and inhibit apoptosis. Han et al [29] also found that silencing ASF1B suppressed the proliferation of prostate cancer cells and promoted their apoptosis and cell cycle arrest, and this inhibitory effect might be related to the inactivation of the PI3K/Akt pathway. This was similar to the results of our study. Our study found that overexpression of ASF1B significantly increased the level of p-AKT, while the inhibition of ASF1B expression had the opposite effect. The PI3K/AKT signaling pathway has been reported to be involved in the regulation of NSCLC proliferation, migration, and epithelial mesenchymal transition (EMT) [30]. Our study also found that the inhibitor of AKT

significantly inhibited the malignant behavior of lung cancer cells, and this inhibitory effect was greatly reduced in ASF1B-overexpressed cells. These data suggested the important role for ASF1B in tumor development. Similar findings can also be seen in the study of Zhang and Wang et al [31]. Our findings once again emphasized that high ASF1B expression predicted a poor prognosis in patients with LUAD, suggesting that ASF1B might also serve as a prognostic marker gene in LUAD.

To further understand the role of ASF1B in LUAD, we further explored the immune-related mechanisms of ASF1B using bioinformatics methods. We found that there were significant correlations between ASF1B and multiple immune cells, as well as immune function or pathways. For example, ASF1B was significantly and positively associated with tumor killer cells (e.g., CD8+ T cells and NK cells) and APC co-inhibition, and Inflammation promoting. In hepatocellular carcinoma [32, 33], ASF1B was also found to be associated with multiple immune-infiltrating cells and immune function signaling pathways, but it was different from our study. They found that ASF1B transcription level was positively linked to the abundance of immune cell infiltration, including CD4+ T cells, DCs, Neutrophils, CD8+ T cells, and B cells. While our study observed that the seven had higher infiltration abundance in the low ASF1B group, including B cells, DCs, iDCs, Mast cells, Neutrophils, TIL, T helper cells. While CD8+ T cells, NK cells, and Th1 cells had higher levels of infiltration in the high ASF1B group. This might indicate that ASF1B had different immune-related roles in different cancer contexts. Given the significant impact of immunotherapy as an emerging treatment in improving the prognosis of cancer patients, we subsequently also investigated the potential association of ASF1B with immunotherapy. Previous studies [19, 34, 35] have revealed the immune checkpoint level, TMB, as well as TIDE in representing the efficacy of immunotherapy. As expected, there was positive correlation between ASF1B expression and immune checkpoint level such as TNRSF9, CD274, PDCD1LG2, LAG3 and PDCD1.

Patients with high ASF1B transcriptional level presented higher TMB as well as lower TIDE score, which already preliminarily suggested that ASF1B might be a potential biomarker to reflect the efficacy of immunotherapy. This inference was reconfirmed in another immunotherapy cohort (IMvigor210). This was also consistent with the findings of the study by Zhang et al. [32]. Interestingly, ASF1B was considered to be associated with immunotherapy efficacy in both hepatocellular carcinoma as well as LUAD, however, the correlation between ASF1B expression and the

abundance of immune cell infiltration was clearly different in these two cancers. This further highlighted the heterogeneity and complexity of the tumor microenvironment.

Overall, our study revealed that ASF1B was overexpressed in LUAD tumor tissues, and was significantly associated with the progression, prognosis, and immunotherapy effect for LUAD. ASF1B might be able to serve as a novel molecular marker to predict patient prognosis and a novel target for tumor therapy. It should be noted that although our data re-emphasize the importance of ASF1B in LUAD, the immune-related mechanisms of ASF1B in LUAD remain unclear, which still need to be intensively investigated in the future.

Abbreviations

ASF1B: histone H3-H4 chaperone anti-silencing function 1B; LUAD: lung adenocarcinoma; TCGA: the Cancer Genome Atlas; GEO: Gene Expression Omnibus; ssGSEA: Single-sample gene set enrichment analysis; TMB: tumor mutation burden; TIDE: tumour immune dysfunction and exclusion; qRT-PCR: Quantitative real-time polymerase chain reaction.

Supplementary Material

Supplementary figures.

<https://www.jcancer.org/v15p0218s1.pdf>

Acknowledgements

This study largely benefited from the large amount of data provided by public databases including GEO, TCGA, HPA, TIMER2, GEPIA2 and so on. We are grateful for the efforts made by the resources and staff to expand and improve the databases.

Funding

This work was supported by grants from the Health Commission of Hubei Province scientific research project, the National Natural Science Foundation of China (No81770095).

Author contributions

Qing Geng and Zhihong Zhao designed the study. Congkuan Song, and Yaolin Song consulted a large number of literature. Xiaoxia Wan designed and drawn the Figures and Tables in the manuscript. Congkuan Song drafted the manuscript. Zhihong Zhao and Qing Geng reviewed and modified this manuscript. All authors read and approved the final manuscript.

Availability of data and materials

The datasets generated and analysed during the current study are available in the TCGA GDC

repository, (<https://portal.gdc.cancer.gov/>), GEO repository, (<https://www.ncbi.nlm.nih.gov/geo/>), Human Protein Atlas (HPA) database (<http://www.proteinatlas.org/>), UALCAN (<http://ualcan.path.uab.edu/>), TIMER2 database (<http://timer.cistrome.org/>), GEPIA2 webserver (<http://gepia2.cancer-pku.cn/>), and TISIDB database (<http://cis.hku.hk/TISIDB/>).

Competing Interests

The authors have declared that no competing interest exists.

References

- Travis W D, Garg K, Franklin W A, Wistuba I I, Sabloff B, Noguchi M, Kakinuma R, Zakowski M, Ginsberg M, Padera R, Jacobson F, Johnson B E, Hirsch F, Brambilla E, Flieder D B, Geisinger K R, Thunnissen F, Kerr K, Yankelevitz D, Franks T J, Galvin J R, Henderson D W, Nicholson A G, Hasleton P S, Roggli V, Tsao M S, Cappuzzo F and Vazquez M. Evolving concepts in the pathology and computed tomography imaging of lung adenocarcinoma and bronchioloalveolar carcinoma. *J CLIN ONCOL*. 2005;23:3279-87.
- Travis W D, Brambilla E, Noguchi M, Nicholson A G, Geisinger K, Yatabe Y, Powell C A, Beer D, Riely G, Garg K, Austin J H, Rusch V W, Hirsch F R, Jett J, Yang P C and Gould M. International Association for the Study of Lung Cancer/American Thoracic Society/European Respiratory Society: international multidisciplinary classification of lung adenocarcinoma: executive summary. *Proc Am Thorac Soc*. 2011;8:381-5.
- Le S, Davis C, Konopka J B and Sternglanz R. Two new S-phase-specific genes from *Saccharomyces cerevisiae*. *YEAST*. 1997;13:1029-42.
- Bao Y and Shen X. Asf1, a loveseat for a histone couple. *CELL*. 2006;127:458-60.
- Peng H, Nogueira M L, Vogel J L and Kristie T M. Transcriptional coactivator HCF-1 couples the histone chaperone Asf1b to HSV-1 DNA replication components. *Proc Natl Acad Sci U S A*. 2010;107:2461-6.
- Messiaen S, Guiard J, Aigueperse C, Fliniaux I, Tourpin S, Barroca V, Allemand J, Fouchet P, Livera G and Vernet M. Loss of the histone chaperone ASF1B reduces female reproductive capacity in mice. *REPRODUCTION*. 2016;151:477-89.
- Paul P K, Rabaglia M E, Wang C Y, Stapleton D S, Leng N, Kendziorski C, Lewis P W, Keller M P and Attie A D. Histone chaperone ASF1B promotes human beta-cell proliferation via recruitment of histone H3.3. *CELL CYCLE*. 2016;15:3191-202.
- Corpet A, De Koning L, Toedling J, Savignoni A, Berger F, Lemaitre C, O'Sullivan R J, Karlseder J, Barillot E, Asselain B, Sastre-Garau X and Almouzni G. Asf1b, the necessary Asf1 isoform for proliferation, is predictive of outcome in breast cancer. *EMBO J*. 2011;30:480-93.
- Chen C, Bao H, Wu L, Chen X, Huang Y, Wang H, Yang Y, Liu J, Lv X and Teng L. ASF1b is a novel prognostic predictor associated with cell cycle signaling pathway in gastric cancer. *J Cancer*. 2022;28;13(6):1985-2000.
- Landi M T, Dracheva T, Rotunno M, Figueroa J D, Liu H, Dasgupta A, Mann F E, Fukuoka J, Hames M, Bergen A W, Murphy S E, Yang P, Pesatori A C, Consonni D, Bertazzi P A, Wacholder S, Shih J H, Caporaso N E and Jen J. Gene expression signature of cigarette smoking and its role in lung adenocarcinoma development and survival. *PLOS ONE*. 2008;3:e1651.
- Selamat S A, Chung B S, Girard L, Zhang W, Zhang Y, Campan M, Siegmund K D, Koss M N, Hagen J A, Lam W L, Lam S, Gazdar A F and Laird-Offringa I A. Genome-scale analysis of DNA methylation in lung adenocarcinoma and integration with mRNA expression. *GENOME RES*. 2012;22:1197-211.
- Rousseaux S, Debernardi A, Jacquiau B, Vitte A L, Vesin A, Nagy-Mignotte H, Moro-Sibilot D, Brichon P Y, Lantuejoul S, Hainaut P, Laffaire J, de Reynies A, Beer D G, Timsit J F, Brambilla C, Brambilla E and Khochbin S. Ectopic activation of germline and placental genes identifies aggressive metastasis-prone lung cancers. *SCI TRANSL MED*. 2013;5:166r-186r.
- Yamauchi M, Yamaguchi R, Nakata A, Kohno T, Nagasaki M, Shimamura T, Imoto S, Saito A, Ueno K, Hatanaka Y, Yoshida R, Higuchi T, Nomura M, Beer D G, Yokota J, Miyano S and Gotoh N. Epidermal growth factor receptor tyrosine kinase defines critical prognostic genes of stage I lung adenocarcinoma. *PLOS ONE*. 2012;7:e43923.
- Okayama H, Kohno T, Ishii Y, Shimada Y, Shiraiishi K, Iwakawa R, Furuta K, Tsuta K, Shibata T, Yamamoto S, Watanabe S, Sakamoto H, Kumamoto K, Takenoshita S, Gotoh N, Mizuno H, Sarai A, Kawano S, Yamaguchi R, Miyano S and Yokota J. Identification of genes upregulated in ALK-positive and EGFR/KRAS/ALK-negative lung adenocarcinomas. *CANCER RES*. 2012;72:100-11.
- Tang H, Xiao G, Behrens C, Schiller J, Allen J, Chow C W, Suraokar M, Corvalan A, Mao J, White M A, Wistuba I I, Minna J D and Xie Y. A 12-gene set

- predicts survival benefits from adjuvant chemotherapy in non-small cell lung cancer patients. *CLIN CANCER RES.* 2013;19:1577-86.
16. Hight S K, Mootz A, Kollipara R K, McMillan E, Yenerall P, Otaki Y, Li L S, Avila K, Peyton M, Rodriguez-Canales J, Mino B, Villalobos P, Girard L, Dospoy P, Larsen J, White M A, Heymach J V, Wistuba I I, Kittler R and Minna J D. An *in vivo* functional genomics screen of nuclear receptors and their co-regulators identifies FOXA1 as an essential gene in lung tumorigenesis. *NEOPLASIA.* 2020;22:294-310.
 17. Shedden K, Taylor J M, Enkemann S A, Tsao M S, Yeatman T J, Gerald W L, Eschrich S, Jurisica I, Giordano T J, Misek D E, Chang A C, Zhu C Q, Strumpf D, Hanash S, Shepherd F A, Ding K, Seymour L, Naoki K, Pennell N, Weir B, Verhaak R, Ladd-Acosta C, Golub T, Gruidl M, Sharma A, Szoke J, Zakowski M, Rusch V, Kris M, Viale A, Motoi N, Travis W, Conley B, Seshan V E, Meyerson M, Kuick R, Dobbin K K, Lively T, Jacobson J W and Beer D G. Gene expression-based survival prediction in lung adenocarcinoma: a multi-site, blinded validation study. *NAT MED.* 2008;14:822-7.
 18. Schabath M B, Welsh E A, Fulp W J, Chen L, Teer J K, Thompson Z J, Engel B E, Xie M, Berglund A E, Creelan B C, Antonia S J, Gray J E, Eschrich S A, Chen D T, Cress W D, Haura E B and Beg A A. Differential association of STK11 and TP53 with KRAS mutation-associated gene expression, proliferation and immune surveillance in lung adenocarcinoma. *ONCOGENE.* 2016;35:3209-16.
 19. Jiang P, Gu S, Pan D, Fu J, Sahu A, Hu X, Li Z, Traugh N, Bu X, Li B, Liu J, Freeman G J, Brown M A, Wucherpfennig K W and Liu X S. Signatures of T cell dysfunction and exclusion predict cancer immunotherapy response. *NAT MED.* 2018;24:1550-8.
 20. Mariathasan S, Turley S J, Nickles D, Castiglioni A, Yuen K, Wang Y, Kadel E I, Koepfen H, Astarita J L, Cubas R, Jhunjhunwala S, Banchereau R, Yang Y, Guan Y, Chalouni C, Ziai J, Senbabaoglu Y, Santoro S, Sheinson D, Hung J, Giltman J M, Pierce A A, Mesh K, Lianoglou S, Riegler J, Carano R, Eriksson P, Hoglund M, Somarriba L, Halligan D L, van der Heijden M S, Loriot Y, Rosenberg J E, Fong L, Mellman I, Chen D S, Green M, Derleth C, Fine G D, Hegde P S, Bourgon R and Powles T. TGFbeta attenuates tumour response to PD-L1 blockade by contributing to exclusion of T cells. *NATURE.* 2018;554:544-8.
 21. Kim S B, Dent R, Im S A, Espie M, Blau S, Tan A R, Isakoff S J, Oliveira M, Saura C, Wongchenko M J, Kapp A V, Chan W Y, Singel S M, Maslyar D J and Baselga J. Ipatasertib plus paclitaxel versus placebo plus paclitaxel as first-line therapy for metastatic triple-negative breast cancer (LOTUS): a multicentre, randomised, double-blind, placebo-controlled, phase 2 trial. *LANCET ONCOL.* 2017;18:1360-72.
 22. Hu X, Zhu H, Zhang X, He X and Xu X. Comprehensive analysis of pan-cancer reveals potential of ASF1B as a prognostic and immunological biomarker. *Cancer Med.* 2021;10:6897-916.
 23. Ma J, Han W and Lu K. Comprehensive Pan-Cancer Analysis and the Regulatory Mechanism of ASF1B, a Gene Associated With Thyroid Cancer Prognosis in the Tumor Micro-Environment. *FRONT ONCOL.* 2021;11:711756.
 24. Liu X, Song J, Zhang Y, Wang H, Sun H, Feng X, Hou M, Chen G, Tang Q and Ji M. ASF1B promotes cervical cancer progression through stabilization of CDK9. *CELL DEATH DIS.* 2020;11:705.
 25. Vasan N, Toska E and Scaltriti M. Overview of the relevance of PI3K pathway in HR-positive breast cancer. *ANN ONCOL.* 2019;30:x3-11.
 26. Song Y, Liu H, Cui C, Peng X, Wang C, Tian X and Li W. Silencing of Peroxiredoxin 1 Inhibits the Proliferation of Esophageal Cancer Cells and Promotes Apoptosis by Inhibiting the Activity of the PI3K/AKT Pathway. *CANCER MANAG RES.* 2019;11:10883-90.
 27. Hong Z, Wang Z, Zhou B, Wang J, Tong H, Liao Y, Zheng P, Jamshed M B, Zhang Q and Chen H. Effects of evodiamine on PI3K/Akt and MAPK/ERK signaling pathways in pancreatic cancer cells. *INT J ONCOL.* 2020;56:783-93.
 28. Zhou F, Geng J, Xu S, Meng Q, Chen K, Liu F, Yang F, Pan B and Yu Y. FAM83A signaling induces epithelial-mesenchymal transition by the PI3K/AKT/Snail pathway in NSCLC. *Aging (Albany NY).* 2019;11:6069-88.
 29. Han G, Zhang X, Liu P, Yu Q, Li Z, Yu Q and Wei X. Knockdown of anti-silencing function 1B histone chaperone induces cell apoptosis via repressing PI3K/Akt pathway in prostate cancer. *INT J ONCOL.* 2018;53:2056-66.
 30. Liu J, Huang B, Xiu Z, Zhou Z, Liu J, Li X and Tang X. PI3K/Akt/HIF-1alpha signaling pathway mediates HPV-16 oncoprotein-induced expression of EMT-related transcription factors in non-small cell lung cancer cells. *J CANCER.* 2018;9:3456-66.
 31. Zhang W, Gao Z, Guan M, Liu N, Meng F and Wang G. ASF1B Promotes Oncogenesis in Lung Adenocarcinoma and Other Cancer Types. *FRONT ONCOL.* 2021;11:731547.
 32. Zhang S, Xu L, Feng J, Tan D, Zhu Y, Hou J, Li W, Lv K, Wang W, Jiang L, Jiao M and Guo H. ASF1B is a Promising Prognostic Biomarker and Correlates With Immunotherapy Efficacy in Hepatocellular Carcinoma. *FRONT GENET.* 2022;13:842351.
 33. Zhan T, Gao X, Wang G, Li F, Shen J, Lu C, Xu L, Li Y and Zhang J. Construction of Novel lncRNA-miRNA-mRNA Network Associated With Recurrence and Identification of Immune-Related Potential Regulatory Axis in Hepatocellular Carcinoma. *FRONT ONCOL.* 2021;11:626663.
 34. Chan T A, Yarchoan M, Jaffee E, Swanton C, Quezada S A, Stenzinger A and Peters S. Development of tumor mutation burden as an immunotherapy biomarker: utility for the oncology clinic. *ANN ONCOL.* 2019;30:44-56.
 35. Cristescu R, Mogg R, Ayers M, Albright A, Murphy E, Yearley J, Sher X, Liu X Q, Lu H, Nebozhyn M, Zhang C, Lunceford J K, Joe A, Cheng J, Webber A L, Ibrahim N, Plimack E R, Ott P A, Seiwert T Y, Ribas A, McClanahan T K, Tomassini J E, Loboda A and Kaufman D. Pan-tumor genomic biomarkers for PD-1 checkpoint blockade-based immunotherapy. *SCIENCE.* 2018;362.